Liquid Crystals
Publication details, including instructions for authors and subscription information:
http://www.informaworld.com/smpp/title~content=t713926090

Imaging of micropatterned self-assembled monolayers with adsorbed liquid crystals

Y. L. Cheng[a]; D. N. Batchelder[a]; S. D. Evans[a]; J. R. Henderson[a]; J. E. Lydon[b]; S. D. Ogier[a]
[a] and Centre for Self-Organising Molecular Systems, University of Leeds, [b] Department of Biochemistry and Molecular Biology, University of Leeds, Department of Physics and Astronomy, Leeds LS2 9JT, UK Leeds LS2 9JT, UK,

Online publication date: 06 August 2010

To cite this Article Cheng, Y. L. , Batchelder, D. N. , Evans, S. D. , Henderson, J. R. , Lydon, J. E. and Ogier, S. D.(2000) 'Imaging of micropatterned self-assembled monolayers with adsorbed liquid crystals', Liquid Crystals, 27: 10, 1267 — 1275
To link to this Article: DOI: 10.1080/026782900423304
URL: http://dx.doi.org/10.1080/026782900423304

LIQUID CRYSTALS, 2000, VOL. 27, NO. 10, 1267–1275

Imaging of micropatterned self-assembled monolayers with adsorbed liquid crystals

Y. L. CHENG, D. N. BATCHELDER, S. D. EVANS*, J. R. HENDERSON, J. E. LYDON† and S. D. OGIER

Department of Physics and Astronomy, and Centre for Self-Organising Molecular Systems, University of Leeds, Leeds LS2 9JT, UK

†Department of Biochemistry and Molecular Biology, University of Leeds, Leeds LS2 9JT, UK

(*Received 12 December 1999; in final form 20 March 2000; accepted 10 April 2000*)

We report a novel method of imaging micropatterned self-assembled monolayers (SAMs) using adsorbed films of thermotropic (smectic or nematic) mesophase which can then be studied by optical microscopy. Three alkylthiols, functionalized with CH_3, OH and COOH groups, were used in various combinations to form patterned SAMs. Two alkylcyanobiphenyls (7CB and 9CB) were used as the liquid crystal imaging reagents. The images are formed by the contrast generated by the different alignments of adsorbed smectic or nematic films induced by different regions of the pattern. The spatial resolution is at least to 4 μm.

1. Introduction

It is with good reason that the liquid crystal (LC) phase has been called Nature's Sensitive Phase. Small changes in external conditions frequently produce readily observable responses. In particular, anyone who has studied the optical microscopy of a nematic phase at first hand will have noticed how readily the director field of the mesophase picks up and highlights any irregularity of a substrate surface. An imperceptible scratch, grease mark or fingerprint on a glass slide will stand out plainly if a layer of nematic phase is placed over it and the sample is then examined between crossed polarizers in a polarizing microscope.

Self-assembled monolayers (SAMs), comprising different ω-functionalized groups, can be used to create surfaces that are patterned with different chemical and physical properties. Patterned SAM surfaces have been widely developed for use in micro-fabrication technology and the study of interfacial phenomena, e.g. wetting, bio-recognition, cell culture, etching, etc [1–5]. The imaging of patterned SAMs requires a sensitivity to chemical composition, since the difference in the molecular structures of the monolayer components is typically small. Techniques for characterization of patterned SAMs, used to date, include scanning electron microscopy (SEM) [6], lateral force microscopy (LFM) [7–9], X-ray photoelectron spectroscopy (XPS) [10], secondary ion mass spectroscopy (SIMS) [11] and surface-enhanced Raman imaging (SERI) [12]. These methods all require sophisticated instruments. In this report, we present a simple, inexpensive way to image patterned SAMs using thermotropic liquid crystals.

The basis of our approach lies in the anchoring properties of nematic and smectic liquid crystals. It is well known that thin liquid crystal films can be oriented by weak surface forces and that this imposed orientation of the liquid crystal director can persist up to tens of μm into a bulk liquid crystal fluid [13, 14]. In recent years, SAMs have been used to manipulate the alignment of liquid crystals at both a lateral and out-of-plane microscale [15–17]. The alignment depends on the combination of chemical functionality, surface energy and roughness [15, 18, 19]. Studies of the surface alignment of liquid crystals can therefore provide information on the composition and wettability of surfaces. Gupta *et al.* have shown that liquid crystals can distinguish between SAMs composed of odd and even number hydrocarbons [20]. They have also used a nematic liquid crystal to optically image ligand–receptor binding [21]. The simplest way to study bulk liquid crystal alignment is polarized optical microscopy. Optical anisotropy, arising from the various preferred orientations of the mesogens, generates different optical textures that may reflect the underlying chemical pattern [15, 22].

*Author for correspondence; e-mail: s.d.evans@leeds.ac.uk

Liquid Crystals ISSN 0267-8292 print/ISSN 1366-5855 online © 2000 Taylor & Francis Ltd
http://www.tandf.co.uk/journals

Standard, calamitic, thermotropic liquid crystals of the cyanobiphenyl family (*n*CB) have been used here to investigate their ability to highlight chemical heterogeneity on patterned SAM surfaces. Previously we have shown that the alignment is dictated by a delicate balance between the length of the alkyl chain of the *n*CB molecules (i.e. intermolecular interactions) and the surface chemical functionality (i.e. the LC surface strength). In particular we found that low energy surfaces (e.g. SAMs functionalized with a CF_3 or CH_3 group) tend to produce homeotropic alignment, whereas higher energy surfaces (e.g. SAMs functionalized with a COOH or OH group) tend to give rise to planar anchoring [16, 19]. Here we present optical images of nematic and smectic liquid crystal films in contact with these patterned SAMs. The resolution and sensitivity of the method is investigated. Lateral force microscopy is used as a complementary technique.

2. Experiments

We have restricted this work to two liquid crystal molecules (7CB and 9CB) and investigated their alignment on chemically heterogeneous substrates. The substrates used here were microcontact-printed SAMs of 11-mercaptoundecanoic acid, 11-mercaptoundecanol and dodecanethiol. These alkylthiols are sufficiently long to form closely packed crystalline monolayers [23].

Smooth gold films were prepared by using the template-stripping method of Stamou *et al.* [24]. Initially, silicon wafers (Laporte Electronics, UK) were cleaned

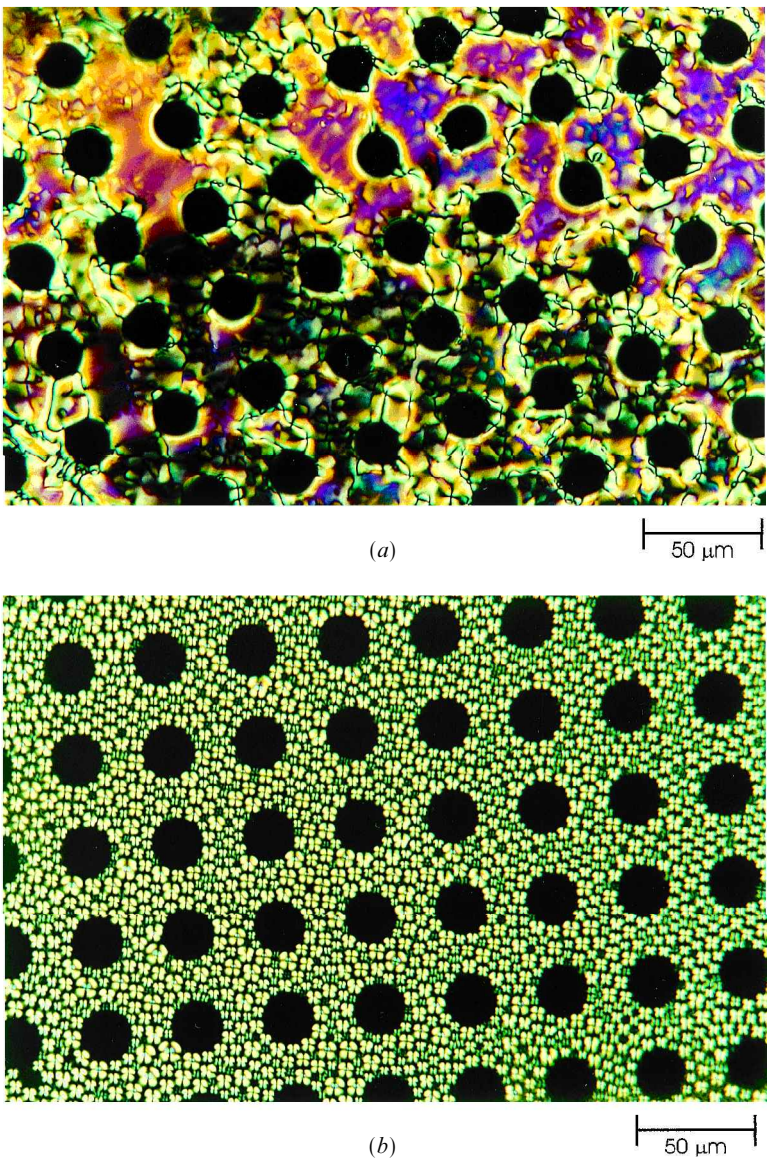

Figure 1. Cross polarized microscope images of 9CB films adsorbed on the patterned substrate SAM(18/40). The circular regions of the substrate were formed with the thiol $CH_3(CH_2)_{11}SH$ and the background from $HOOC(CH_2)_{10}SH$. The diameter of each circle is 18 μm and the spacing between them (centre-to-centre) is 40 μm. (*a*) Nematic 9CB at 50.3°C; (*b*) smectic 9CB at 47.0°C.

by sequential sonication in Milli-Q water, methanol, dichloromethane, and methanol. The Si wafers were then dried in a stream of N_2 before being placed in the chamber of an Edwards Auto 306 TMP vacuum evaporator. Au films (99.99%, ADVENT, UK), 200 Å thick, were deposited at a base pressure $< 2 \times 10^{-6}$ mbar. The substrates were then removed from the chamber. A glass slide was glued onto the Au surface using EPO-TEK377 (Promatech Ltd., UK) and the samples were cured at 150°C for 2 h. Finally, the Au/glass substrates were separated from the silicon wafers to leave smooth, clean Au surfaces.

Patterned SAMs were prepared by microcontact printing [25, 26]. Poly(dimethylsiloxane) elastomer stamps (patterned as an array of circular indents with diameters between 2 and 18 μm) were inked with 5mM ethanol solutions of $HOOC(CH_2)_{10}SH$ (Aldrich, UK) and placed in contact with the gold films. After 30 s each substrate was immersed for ~1 min in a 1mM solution of $CH_3(CH_2)_{11}SH$ (Aldrich, UK) in ethanol. The substrates were subsequently rinsed in ethanol and dried under a stream of filtered N_2. The resultant patterned SAMs consisted of circular regions of CH_3-functionalized monolayer, on a background of COOH monolayer (denoted CH_3/COOH). Additional classes of patterned SAMs, including OH/COOH, and a mixed (CH_3/COOH)/COOH system, were prepared in a similar fashion.

The thin layer of liquid crystal (Merck Ltd., UK) was formed by placing several pieces of the solid mesogen on the SAM surface. The sample was then heated into

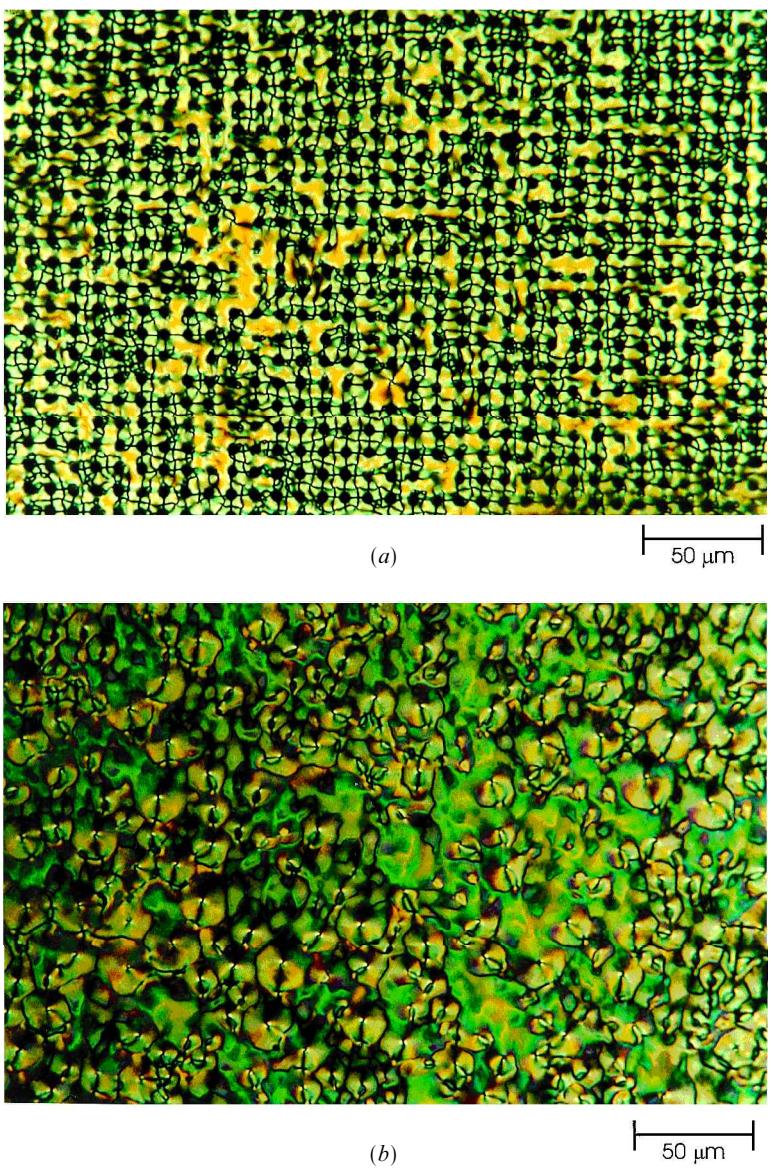

Figure 2. Cross polarized microscope images of nematic 9CB films, at 50.3°C, adsorbed on patterned substrates. The circular regions of the substrates were formed with the thiol $CH_3(CH_2)_{11}SH$ and the background from $HOOC(CH_2)_{10}SH$. (*a*) SAM(4/10); (*b*) SAM(2/10).

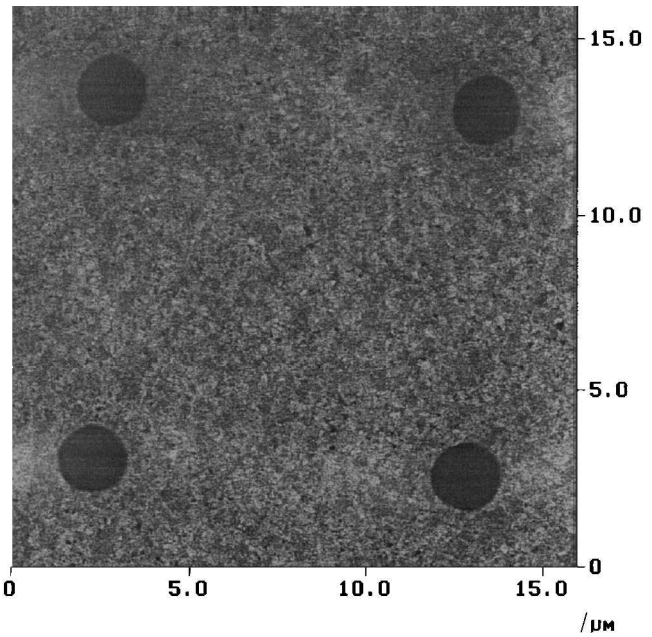

Figure 3. A lateral force microscopy image of the patterned SAM(2/10) used to obtain figure 2(*b*). The image was taken at ambient conditions with a Z range of 0.5 V.

the isotropic phase at which point a clean glass cover slip was placed onto the melted LC to ensure uniform coverage of the sample. The cover slip was subsequently removed, whilst the LC was still in its isotropic phase, to leave a 'free' LC surface. Our analysis below assumes that subsequent 'dewetting' of LC on hydrophobic regions did not take place.

A BH2 Olympus polarizing microscope was used to observe the optical textures. All images were obtained with white light at a magnification of 400×, achieved using a combination of a 40× objective lens with a second 10× magnifying lens situated between the camera and the objective lens. A Linkam hot stage was used to vary sample temperatures, at a rate of 5°C min^{-1}, with an accuracy of ± 0.1°C.

The lateral force imaging was obtained using a Molecular Imaging™ pico SPM controlled with nanoscope III electronics (Digital Instruments, USA). A short, narrow-legged, triangular, silicon nitride cantilever (nominal spring constant of 0.32 N m^{-1}, Digital Instruments, USA) was used. The scan angle was set perpendicular to the major axis of the cantilever. The measurements were taken in air at room temperature, at a scan rate of 2 Hz.

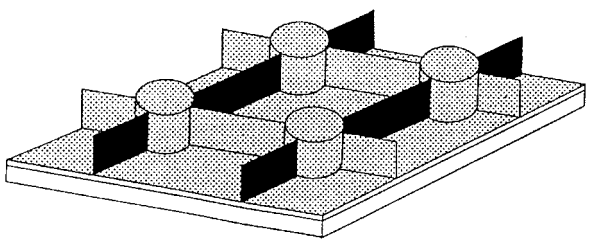

(a)

(b) (c)

(d) (e)

Figure 4. The ideal texture of the nematic film. In these sketches the lines indicate the nematic director, i.e. the alignment of the long axes of the molecules. In the circular homeotropic regions we picture the molecules lying perpendicular to the substrate. The director field is divided into cells, although the pattern of figure 1(*a*) is far from perfect. When compared with figure 2(*a*) one is led to define the appearance of an idealized cell. We interpret this pattern in terms of the structure shown in (*a*)–(*e*). Each cell is bounded by vertical disclination walls of homeotropic alignment as sketched in (*a*). In the intervening regions, the nematic phase forms a closed pattern, as if spherical polar droplets (*b*) have been distorted by forcing them to fit into a tray divided into shallow square boxes (*c*). The appearance of the sample between crossed polarizers does not distinguish between the structures shown in (*d*) (with homeotropic anchoring at the upper surface) and that shown in (*e*) (with planar anchoring at the upper surface), since both patterns have the same projection in the plane of the surface.

3. Results and discussion

Figure 1 shows the optical textures observed for 9CB, in its nematic (*a*) and smectic (*b*) phases, in contact with a patterned SAM. The substrate pattern is formed from circular islands of a CH_3-functionalized monolayer within a background of COOH monolayer. The diameter of the circular regions is 18 μm and their centre-to-centre distance is 40 μm. We therefore designate this surface as SAM(18/40). Both images clearly display the pattern, with a higher contrast obtained from the image of smectic 9CB. The colourful texture between the CH_3 islands implies that in these regions the LC is aligned planar (or perhaps partially tilted) with respect to the surface. As there is no specific directional treatment to the substrates, we picture the planar aligned molecules as being free to take up whichever orientation parallel to the surface gives the lowest energy for the director field as a whole. The dark circles, where the polarized light is extinguished completely, imply that the LC alignment in these regions is homeotropic. This agrees with an evanescent wave ellipsometry study, for temperatures in the vicinity of the isotropic to nematic phase transition, that has shown that 9CB is homeotropically anchored on the pure CH_3 substrate, but is planar aligned when in contact with the COOH monolayer [19].

To investigate the spatial resolution of our imaging technique, we prepared additional substrates denoted SAM(4/10) and SAM(2/10) using the same designation introduced above. Figure 2 displays the optical textures of nematic 9CB, in contact with these substrates. One can clearly see the 4/10 pattern (*a*), although there are some bright patches in the image due to non-uniformity of the LC film. At this magnification the image of nematic 9CB on the 2/10 patterned SAM (*b*) does not show an underlying substrate pattern. To confirm that SAM(2/10) really is patterned, we used lateral force microscopy (LFM) to image the SAM (figure 3). The darker circular regions, where friction is low, confirm the presence of CH_3-functionalized monolayer. The brighter background, where friction is higher, corresponds to a COOH monolayer, as expected.

A tentative explanation of the ideal nematic texture, seen more clearly in figure 2(*a*), is given in figures 4 and 5. The director field is divided into cells with each cell bounded by vertical disclination walls of homeotropic alignment, figure 4(*a*). In the circular homeotropic region, the molecular long axes of the mesogens are depicted lying perpendicular to the substrate. In the intervening region, the director lies parallel to the bottom surface as if a spherical polar droplet, figure 4(*b*), has been

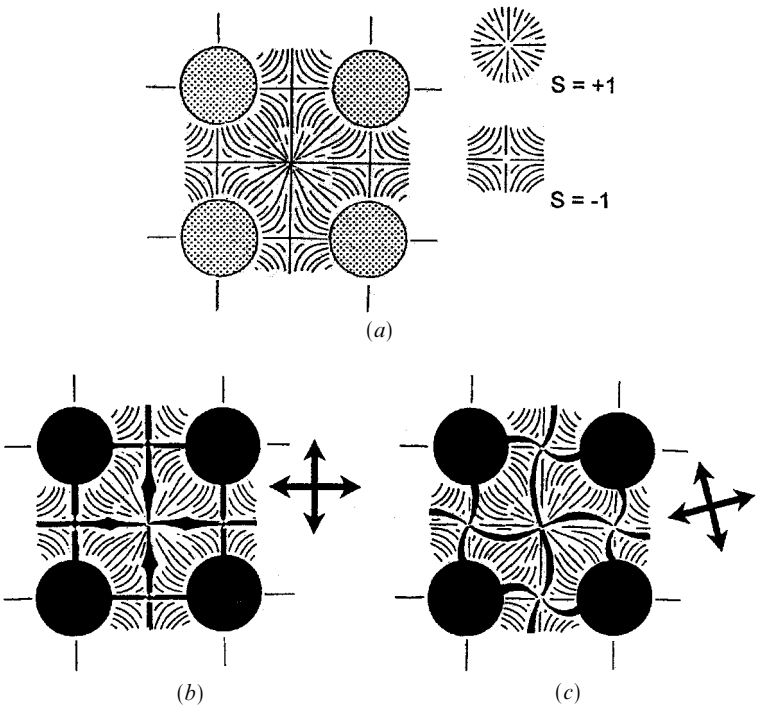

Figure 5. The normal view of the director field of the texture. The sketch shown in (*a*) represents the director field when the ideal nematic sample is viewed normal to the surface. There is an alternating array of disclinations. At the centre of each unit there is a disclination of strength +1 and at a position half way along the sides, there are disclinations of strength −1. Figures 5(*b*) and (*c*) explain the way in which the appearance of the extinction lines would change if the ideal sample was rotated between crossed polarizers; cf. the fluctuations seen in figure 2(*a*).

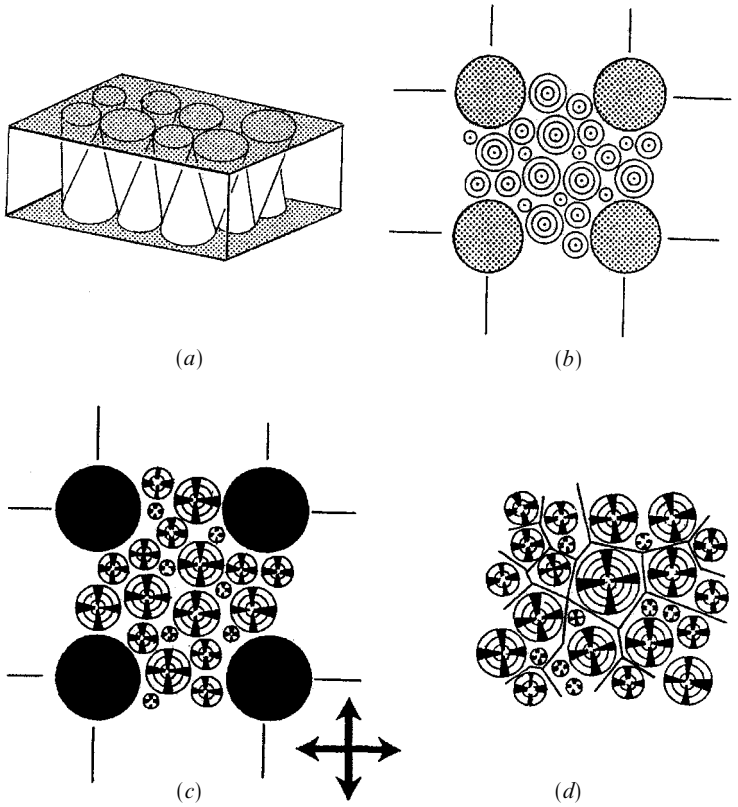

Figure 6. The texture of the smectic film. In this group of figures the construction lines indicate the alignment of the surfaces of the smectic layers. The director is divided into circular domains and we interpret these in terms of an array of focal conic units as depicted in (*a*). The projection of this structure viewed down the axes of the conics is shown in (*b*). Between crossed polarizes, a sample with this structure will have the multispherulite appearance of extinction lines shown in (*c*). This texture is similar to that of the familiar smectic 'polygonal' texture, but note that it lacks the distinct straight line disclinations grouping the circular regions into polygons, as sketched in (*d*). We observed that as the focus was raised (lowered) in figure 1 (*b*) all the circular regions swelled (shrank), rather than alternate circles shrinking and swelling as assumed in sketch (*a*). Perhaps our image is dominated by focusing in the region of the upper surface.

distorted by forcing it to fit into a cell, figure 4 (*c*). Top views of the nematic director field of the ideal texture are given in figure 5.

For the smectic 9CB image, figure 1 (*b*), the alignment on CH_3 regions remains homeotropic, while the texture on COOH regions changes from schlieren to 'polygonal'. The director field of planar alignment is now divided into circular domains and we interpret these in terms of an array of focal conic units as depicted in figures 6 and 7. In each homeotropic region, a parallel stack of smectic layers extends vertically throughout the mesophase. Between these stacks, the bulk of the mesophase is filled with focal-conic domains. Since the smectic phase was formed by cooling the sample from the nematic phase, it might have been expected that the smectic pattern would have retained the simple one-domain-per-unit-cell features of nematic samples such as figure 2 (*a*). However, this was not found to be the case and the probable reason is sketched in figure 8.

The high contrast images discussed above arose from a choice of functionalized groups associated with opposite anchoring conditions. However, even when the anchoring remains planar on both regions of the pattern, one might still expect some contrast due to the different anchoring strengths. In this way, adsorbed liquid crystals could display sensitivity to surface energy [27]. To investigate this possibility we constructed two further patterned SAM(18/40) substrates. One (PS1) was formed from an OH-functionalized monolayer (circular regions) on a COOH background, while the other (PS2) was composed of randomly mixed CH_3(20%)/COOH(80%) monolayer (circular regions) on a COOH background†

† The quoted percentage of the mixed CH_3/COOH SAM is the concentration of the bulk thiol solution, and is thus only a qualitative guide to the surface composition. Calibration is possible via X-ray photoelectron spectroscopy, but was not required for this study.

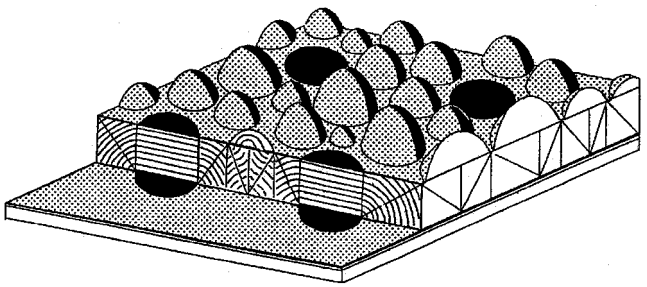

Figure 7. The proposed structure of the smectic layer. This sketch shows the postulated arrangement of layers within the film of smectic mesophase, such as that shown in figure 1 (*b*). The homeotropic regions are pictured as giving rise to parallel stacks of smectic layers extending vertically throughout the mesophase, like stacks of pancakes. Between these stacks, the bulk of the mesophase is filled with focal conic domains. The lower part of this structure corresponds to a conventional polygonal texture, but we would expect that the free upper surface may have some additional detail depending on the free surface anchoring condition. For a homeotropic upper surface, we propose therefore that half-onion hemispheres cap the focal conic units with upward facing bases giving a cobbed rather than a flat surface (as drawn).

[28]. We found that nematic 7CB imaged these patterned SAMs better than nematic or smectic 9CB. Figures 9 (*a*) and 9 (*b*) display the resulting nematic 7CB optical images. The contrast is not as good as in figure 1 and the edges of the circular regions are optically rougher than the underlying molecular pattern. Nevertheless, the patterns are clearly visible, despite the fact that 7CB shows planar anchoring on unpatterned substrates of any of these OH, CH_3 and mixed CH_3/COOH, functionalized monolayers [19]. The difference in advancing water contact angle between the mixed CH_3(20%)/COOH(80%) and COOH monolayers is 30°, so there is a significant surface free energy contrast for substrate PS2. However, both OH- and COOH-functionalized SAMs are hydrophilic (advancing water contact angles $\sim 10°$). The fact that the LC can image our OH/COOH patterned SAM shows that there is a subtle difference in the anchoring free energy which a contact angle for water drops cannot detect.

4. Conclusion

This study demonstrates that micropatterned SAMs can be optically imaged using thin layers of adsorbed thermotropic liquid crystals. Although the spatial resolution is lower than that of lateral force microscopy, there are obvious advantages to our procedure at micron scale resolution: (i) the technique is non-destructive as the liquid crystals can be easily rinsed off with a solvent,

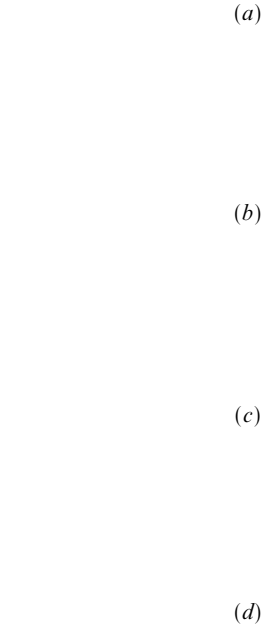

Figure 8. The relationship between the nematic and smectic textures. The nematic director field across the diagonal of figure 4 (*d*) is sketched in (*a*). The smectic structure derived from this (by drawing smectic layers perpendicular to the nematic director) is shown superimposed in (*b*) and on its own in (*c*). Note that this pattern is not a particularly stable arrangement since it contains a large amount of splay and has a large Gaussian curvature. Presumably it is so energetically unfavourable that it spontaneously reverts to the focal conic structure shown in (*d*), which has zero Gaussian curvature. (Note, depicted here is the way in which each smectic cell appears to revert to random groups of focal-conic units, see figures 6 and 7.)

(ii) it is a very simple and inexpensive procedure. We believe that this method can be used, in general, to map micro or larger scale heterogeneous (chemical or structural) surfaces. This will provide valuable additional information to the more conventional contact angle measurement analysis of surfaces using adsorbed drops of isotropic test liquids. The latter technique has proved to be of great practical significance to a wide variety of technologies associated with wetting phenomena [27–29]. However, this approach to characterize surface properties is problematic for chemically heterogeneous/patterned surfaces, because it is difficult to ensure that the adsorbed drops statistically sample the entire pattern and, if not, whether pinning of the contact line at chemical boundaries will lead to violations of Young's equation [30, 31].

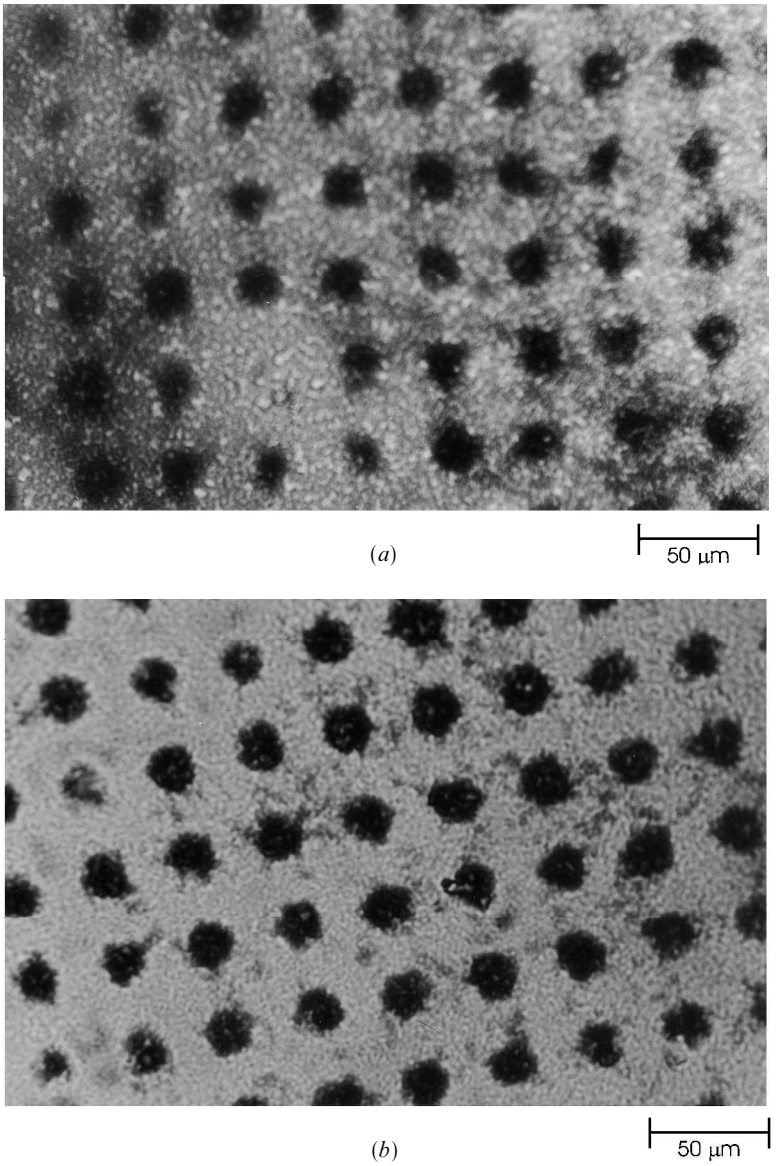

Figure 9. Cross polarized, black and white microscope images of nematic 7CB films, at 35.0°C, adsorbed on two examples of a patterned SAM(18/40). (*a*) PS1: the circular regions were formed with the thiol $OH(CH_2)_{10}SH$ and the background from thiol $HOOC(CH_2)_{10}SH$; (*b*) PS2: the circular regions were formed with a mixed thiol solution of 20% $CH_3(CH_2)_{11}SH$ and 80% $COOH(CH_2)_{10}SH$, on the same background as PS1.

From a technological point of view, as far as we are aware, all present-day liquid crystal display devices involve substrate surfaces giving large areas of uniform alignment and any tendency of the mesophase to form a mosaic of domains would clearly be a detrimental nuisance. However, we suggest that a new and more sophisticated type of device is possible where the intrinsic domain-forming properties of the mesophase are matched to details on the substrate surfaces. This would give controllable highly-patterned textures which may well have attractive commercial features.

This work is supported by the EPSRC. We would like to thank Dr Jin Zhang for assistance with the lateral force microscopy.

References

[1] Clark, S. L., Montague, M., and Hammond, P. T., 1997, *Supramol. Sci.*, **4,** 141.
[2] Wilbur, J. L., Kumar, A., Biebuyck, H. A., Kim, E., and Whitesides, G. M., 1996, *Nanotech.*, **17,** 452.
[3] Kumar, A., and Whitesides, G. M., 1993, *Appl. Phys. Lett.*, **63,** 2002.
[4] Lea, A. S., Pungor, A., Hlady, V., Andrad, J. D., Herron, J. N., and Voss, E. W., Jr., 1992, *Langmuir*, **8,** 68.
[5] Mrksich, M., Dike, L. E., Tien, J., Ingber, D. E., and Whitesides, G. M., 1997, *Exp. Cell. Res.*, **235,** 305.
[6] Lopez, G. P., Biebuyck, H. A., and Whitesides, G. M., 1993, *Langmuir,* **9,** 1513.
[7] Wilbur, J. L., Biebuyck, H. A., MacDonald, J. C., and Whitesides, G. M., 1995, *Langmuir*, **11,** 825.
[8] Hayes, W. A., Kim, H., Yue, X., Perry, S. S., and Shannon, C., 1997, *Langmuir*, **13,** 2511.

[9] Zhou, Y., Fan, H., Fong, T., and Lopez, G. P., 1998, *Langmuir*, **14,** 660.
[10] Lopez, G. P., Biebuyck, H. A., Harte, P., Kumar, A., and Whitesides, G. M., 1993, *J. Am. chem. Soc.*, **115,** 10 774.
[11] Frisbie, C. D., Martin, J. R., Duff, R. R. J., and Wrighton, M. S., 1992, *J. Am. chem. Soc.*, **114,** 7142.
[12] Tryk, D. A., Yang, X. M., Hashimoto, K., and Fuhishima, A., 1998, *Bull. chem. Soc. Jpn.*, **71,** 31.
[13] Cognard, J., 1982, *Mol. Cryst. liq. Cryst. suppl.*, **1,** 1.
[14] Jerome, B., 1991, *Rep. Prog. Phys.*, **54,** 391.
[15] Drawhorn, R. A., and Abbott, N. L., 1995, *J. phys. Chem.*, **99,** 16 511.
[16] Evans, S. D., Allinson, H., Boden, N., and Henderson, J. R., 1996, *Faraday Dissuss.*, **104,** 37; Evans, S. D., Allinson, H., Boden, N., Flynn, T. M., and Henderson, J. R., 1997, *J. phys. Chem. B*, **101,** 2143; Cheng, Y. L., Batchelder, D. N., Evans, S. D., and Henderson, J. R., 1998, *J. phys. Chem. B*, **102,** 5309.
[17] Gupta, V. K., and Abbott, N. L., 1997, *Science*, **276,** 1533.
[18] Ruths, M., Steinberg, S., and Israelachvili, J. N., 1996, *Langmuir*, **12,** 6637.
[19] Alkhairalla, B., Allison, H., Boden, N., Evans, S. D., and Henderson, J. R., 1999, *Phys. Rev. E*, **59,** 3033.
[20] Gupta, V. K., Miller, W. J., Pike, C. L., and Abbott, N. L., 1996, *Chem. Mater.*, **8**, 1366; Gupta, V. K., and Abbott, N. L., 1999, *Langmuir*, **15,** 7213.
[21] Gupta, V. K., Skaife, J. J., Dubrovsky, T. B., and Abbott, N. L., 1998, *Science*, **279,** 2077.
[22] Demus, D., and Richter, L., 1978, *Textures of Liquid Crystals* (Weinheim: VCH).
[23] Chidsey, C. E., and Loiacono, D. N., 1990, *Langmuir*, **6,** 682.
[24] Stamou, D., Gourdon, D., Liley, M., Burnham, N. A., Kulik, A., Vogel, H., and Duschl, C., 1997, *Langmuir*, **13,** 2425.
[25] Kumar, A., Biebuyck, H. A., and Whitesides, G. M., 1994, *Langmuir*, **10,** 1498.
[26] Kumar, A., Abbott, N. L., Kim, E., Biebuyck, H. A., and Whitesides, G. M., 1995, *Acc. chem. Res.*, **28,** 219.
[27] Zisman, W. A., 1964, *Adv. Chem. Ser.*, **43,** 1.
[28] Cassie, A. B. D., 1948, *Discuss. Faraday Soc.*, **3,** 11.
[29] Drummond, C. J., and Chan, D. Y. C., 1997, *Langmuir*, **13,** 3890.
[30] Henderson, J. R., 2000, *Mol. Phys.*, **98,** 677.
[31] Gau, H., Herminghaus, S., Lenz, P., and Lipowsky, R., 1999, *Science*, **283,** 46.